

Shear Performances of Hybrid Notch-Screw Connections for Timber-Concrete Composite Structures

Benkai Shi,^a Yongqing Dai,^a Haotian Tao,^b and Huifeng Yang^{a,*}

This paper presents the push-out experimental results of hybrid notch-screw (HNS) connections for timber-concrete composite structures. A total of 7 groups of specimens were designed and tested. The experimental parameters included the loading constraint conditions (*i.e.*, the test specimens were loaded either in local compression or in uniform compression), shapes of notches in the wood, screw number in notch, notch width, and the inclusion of a self-tapping screw reinforcement for timber or not. The experimental results were discussed in terms of failure modes, ultimate strength, slip moduli, and ductility. The yield strengths and ductility factors were determined based on the load-slip curves according to existing standards. The experimental results showed that both the shear timber width and the self-tapping screw reinforcement played important roles in terms of the ultimate strengths, ductility, and deformability. Rectangular notched connections with screw reinforcements displayed timber shear failure coupled with brittle failure. With the trapezoidal notch, the ductility of the connections improved, coupled with a decrease in the slip modulus. The self-tapping screw reinforcement for shear timber could greatly improve the ductility performance of the HNS connections. The slip modulus models for the connection with vertical deep notches were provided, which were in agreement with the experimental results.

DOI: 10.15376/biores.17.2.2259-2274

Keywords: Timber-concrete composite; Hybrid notch-screw connection; Ductility; Slip modulus; Push-out tests

Contact information: a: College of Civil Engineering, Nanjing Tech University, Nanjing 211816 China;

b: School of Civil Engineering, Southeast University, Nanjing 211189 China;

* Corresponding authors: hfyang@njtech.edu.cn; yhfblon@163.com

INTRODUCTION

Timber-concrete composite (TCC) structures are composed of upper concrete slabs, bottom timber beams/floors, and shear connections. This type of composite structure was developed for the refurbishment of old timber buildings and newly built residential and commercial buildings. Some investigations have been performed to compare the shear behaviors of HNS connection to other connection types. Existing investigations demonstrated that HNS connections showed better shear capacities and slip moduli than traditional screw and metal tooth plate connections (Yeoh *et al.* 2010; Dias *et al.* 2018a).

In addition, the influences of notch geometries on the shear performances of HNS connections have been further investigated. Yeoh *et al.* (2009) investigated HNS connections with different notch shapes, including rectangular, slant, and curve notches. The testing results showed that the connections with rectangular notches yielded an approximately 40% improvement in the slip stiffness compared with the slip stiffness with curve notches, and the load-carrying capacity slightly decreased with the increase of the

inclination angle for slant notches connection. Xie *et al.* (2017) researched the influence of the dimensions of both the grooves and studs in groove-stud connectors and found that increasing the groove area only leads to an increased slip modulus, which has no obvious influence on the ultimate strength while the dimension of the groove was sufficient. Similarly, Auclair *et al.* (2016) proposed an innovative connector for TCC structures, composed of a concrete shell and a steel core, and found that the connector primarily failed due to the shear failure of the concrete shell and the yielding of the steel core. Djoubissie *et al.* (2018) investigated the mechanical behaviours of notched connections with threaded reinforcing bars and found that the triangular notched connection with a 120° threaded bar inclination showed an improvement of 22% in maximum failure loads and 28% in initial slip stiffness compared to those with vertical threaded bars.

The failure mechanisms of both the HNS connections and the associated TCC beams/floors have been research emphases in various available investigations. Boccadoro *et al.* (2017a,b) proposed analysis models to calculate the potential failure modes of TCC structures with notched and HNS connections. The pure notched connection without screws primarily showed brittle shear failure of concrete tenons, and the introduction of screws/studs considerably improved the shear performance of the HNS connections (Djoubissie *et al.* 2018). According to the suggestions of the report of COST Action FP 1402, the minimum requirements for the notch depth for building and bridge applications are 20 mm and 50 mm, respectively (Dias *et al.* 2018b). With an increase in the notch depth, the slip moduli and ultimate bearing capacity increased correspondingly. However, the failure mode turned to timber brittle shear failure for the connection with deep notches, compared to the timber crushing failure found with shallow notches, and the ductility behaviour also gradually decreased (Mönch and Kuhlmann 2018; Zhang *et al.* 2020). Timber shear failure parallel to the grain was also the primary failure mode in full-scale TCC beam, which greatly effects the application of deep notches (Shi *et al.* 2020). Although Lamothe *et al.* (2020) proposed a ductile notch connection based on ultra-high performance fiber reinforced concrete, the ductile problem for notched connections with ordinary concrete still should be further researched; a similar connection with ordinary concrete demonstrated that the brittle failure of concrete and timber are still not solved. (Müller and Frangi 2021). Based on the failure mechanisms mentioned above, the load-carrying capacity calculation methods were provided in the existing design methods (Dias *et al.* 2018; Auclair 2020). However, reliable estimation models for the slip modulus of HNS connections needs to be further investigated.

As previously mentioned, the slip modulus model and ductility of HNS connections with a deep notch need to be further investigated. The ductility of HNS connections will greatly influence the application of TCC structures in multi-story timber buildings, especially in areas with relatively high seismic precautionary requirements. Therefore, the purposes of this research program were to obtain effective improvement measures for hybrid deep notch and screw connections in terms of the shear strength, ductility, and slip moduli models to solve the local failure issues of TCC beams caused by the brittle failure of the HNS connections (Shi *et al.* 2021b).

This experimental program was conducted in two phases: a preliminary phase (Phase I) and an in-depth research phase (Phase II). Push-out tests were adopted to evaluate the shear performances of the HNS connections according to EN standard 26891 (1991). The tests in Phase I were performed to investigate the typical failure modes of HNS connections with a rectangular deep notch. The research parameters included the screw number and loading constraint conditions. Based on the failure modes seen in the Phase I

tests, some improvement solutions were proposed in Phase II. The research parameters included the notch shape, timber shear width, and self-tapping screw reinforcement. The improvement solutions obtained the desired results in terms of the ultimate bearing capacity, deformability, and ductility, which effectively improved the brittle shear failure of HNS connections. The estimating models for the slip moduli at serviceability limit states were proposed were in agreement with the experimental results. The research results of this article have potential to provide guidance for the application of HNS connections in TCC structures.

EXPERIMENTAL

Materials

The timber adopted in this research program was Douglas fir glued laminated timber (glulam). The timber used in the Phase I and Phase II tests was made by from same batch of dimension lumber pieces. The compression strength and elasticity modulus of the timber parallel to grain were tested according to EN standard 408 (2009). The average elasticity modulus of the glulam in Phase I and Phase II were tested as 12900 MPa and 13000 MPa, respectively, while the compressive strengths were tested as 36.8 MPa and 34.7 MPa, respectively. The shear strength of the dimension lumber parallel to the grain was tested in accordance with ISO standard 3347 (1976). The shear strength of the bond line was tested according to ASTM standard D905 (2013). The average values of the material properties tested are displayed in Table 1. The material properties of the timber used in the two-phase experiments were essentially same as the adoption of the same batch of dimension lumber pieces.

Table 1. Material Properties of the Timber Parallel to Grain (MPa)

Phase	Modulus of Elasticity	Compressive Strength	Shear Strength of the Timber	Shear Strength of the Bond Line
Phase I	12900	36.8	6.0	10.4
Phase II	13000	34.7	6.2	9.5

Hexagon head coach screws were adopted for the HNS connections. As shown in Fig. 1a, the diameter and length were 16 mm and 180 mm, respectively. To prevent timber cracking, a prebored hole with a diameter of 12 mm was pre-formed. The average bending yield strength was found to be 300.9 MPa, according to ASTM standard F1575 (2017). Self-tapping screws (VGZ7140 series) were adopted to strengthen the shear of the timber. As shown in Fig. 1b, the dimensions of the self-tapping screws were 7 mm for the nominal diameter and 140 mm in length. The shank and tip diameter were 5 mm and 4.6 mm, respectively. The diameter of the pre-drilling hole for the self-tapping screw was 4 mm. The characteristic yield moment of the self-tapping screw was 14200 MPa, as provided by the manufacturer (Rothoblaas 2019).

The concrete adopted in this experimental research was grade C30/35. The average compressive strengths of the standard cubic specimens (150 mm × 150 mm × 150 mm) during the Phase I and Phase II tests were 42.8 and 40.8 MPa, respectively, at the age of 28 d under natural conservation conditions. The reinforcement rebars adopted in this experimental program were made of hot-rolled rebars, with a standard nominal yield strength of 345 MPa.

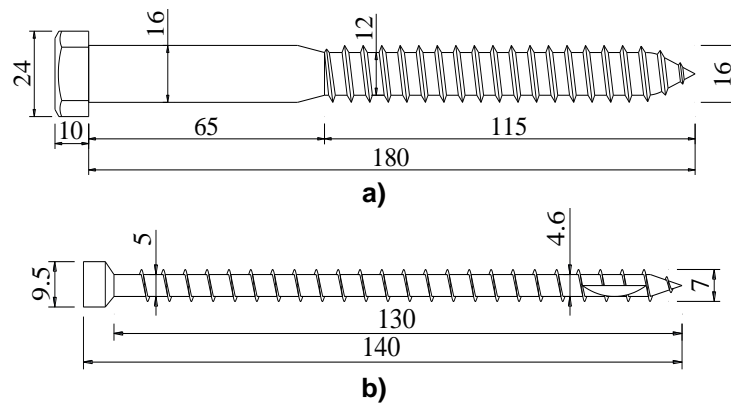


Fig. 1. Dimensions of the screws: a) the coach screw in the notch; and b) the reinforcement screw (Note: both are measured in mm)

Sample Preparation

The overall geometry of a push-out specimen is shown in Fig. 2. The symmetrical configuration of concrete-timber-concrete was adopted in the push-out tests. The steel rebar mesh was buried in the concrete slab while pouring the concrete. The diameter of the rebar was 8 mm, while the center distance was 100 mm. The moisture content of the dimension lumber was lower than 12% while the glulam was constructed. The curing periods of the concrete for the specimens in Phase I and Phase II were approximately 3 months and 1 month, respectively, while the push-out specimens were tested.

The grouping and configurations of the shear connections are displayed in Table 2. Typical photographs of the notched timber blocks are shown in Fig. 3. As shown in Fig. 3b, two VGZ7140 self-tapping screws were applied to strengthen the shear plane of the timber block for the HRSS(R) specimens. For the TSS and HTSS specimens, the slant angle corresponding to the vertical line was 45° . The penetration depth of the screw was 80 mm.

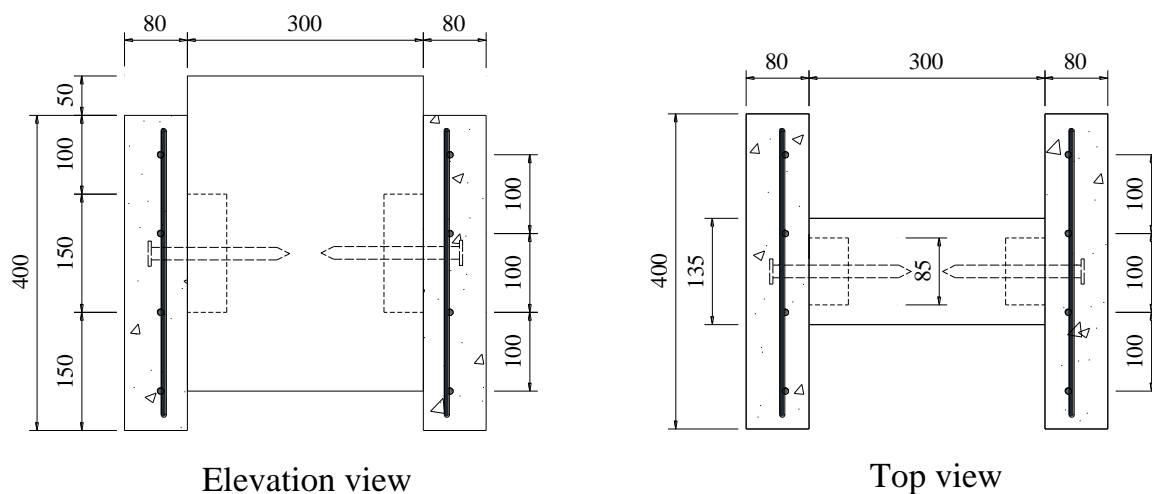


Fig. 2. Schematics of a push-out specimen (Note: the measurements are in mm)

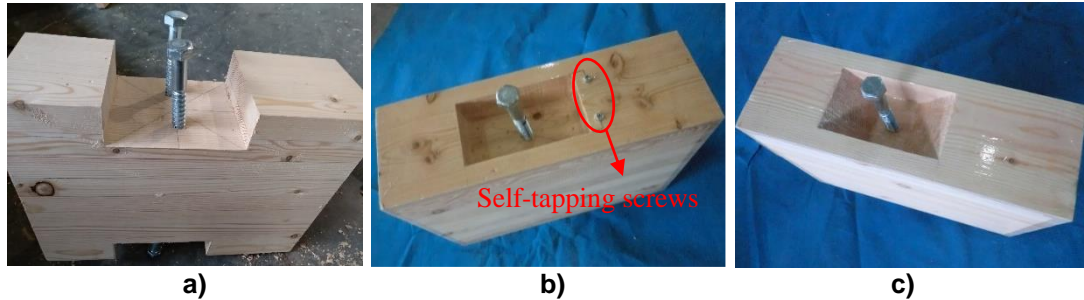


Fig. 3. The timber notches combined with screws: a) RDS; b) HRSS(R); and c) HTSS

Table 2. Configuration Description of the Push-Out Specimens

Group	Notch Shape	Notch Width (mm)	Screw Number	Reinforcement Screw for Timber	Phases	No.
RSS	Rectangle	135	1	None	I	3
RSS(C)	Rectangle	135	1	None	I	3
RDS	Rectangle	135	2	None	I	3
HRSS	Rectangle	85	1	None	II	5
HRSS(R)	Rectangle	85	1	2	II	5
TSS	Trapezoid	135	1	None	II	5
HTSS	Trapezoid	85	1	None	II	5

Note:

1. The depth and length of the HNS connections were uniformly 50 mm and 150 mm, respectively.
2. RSS denotes the rectangular notch with single screw.
3. The only difference between the specimens in groups RSS and RSS(C) is that the former was loaded in local compression, while the latter was loaded in uniform compression.
4. RDS denotes the rectangular notch with double screws.
5. HRSS refers to rectangular hemi-notch with single screw.
6. HRSS(R) denotes rectangular hemi-notch with single screw and reinforced by self-tapping screws.
7. TSS means the trapezoidal notch with single screw.
8. HTSS denotes trapezoidal hemi-notch with single screw.

Testing Methods

The testing set-ups for the push-out tests are illustrated in Fig. 4. The RSS(C) samples were tested using the testing set-up in Fig. 4b, while other samples were tested using the testing set-up in Fig. 4a. For the testing set-up shown in Fig. 4a, the push-out specimen was covered partially by the steel-plate of the actuator. The distance from the end of the steel plate to the end of the timber block was 50 mm. The timber block in the testing set-up shown in Fig. 4b was completely covered by the steel plate. The relative slips between the timber block and the concrete slabs were recorded *via* four linear voltage displacement transducers (LVDTs). The push-out tests were performed in accordance with the loading procedure specified in EN standard 26891 (1991).

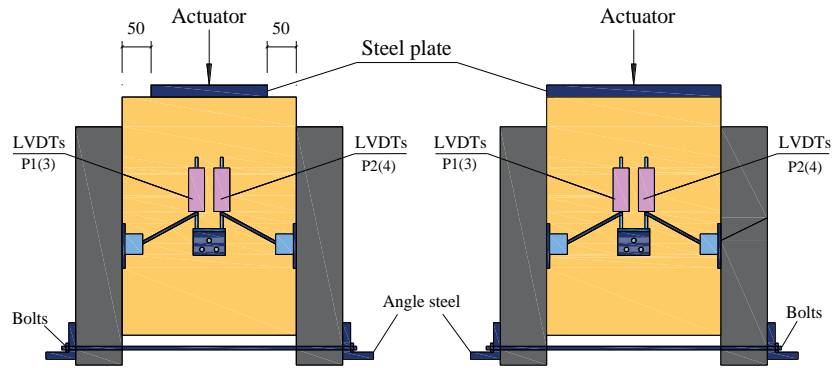


Fig. 4. Test set-up of the push-out tests: a) group RSS in local compression; and b) group RSS(C) in uniform compression. (Note: the measurements are in mm)

RESULTS AND DISCUSSION

Failure Modes

The failure photographs of the specimens tested in Phase I are shown in Fig. 5. The primary failure mode of the RSS and RDS specimens was shear failure of the timber block parallel to the grain. The timber block was sheared out along the bottom of the timber notch coupled with the brittle failure, whereas the concrete tenon was intact. The RSS(C) specimens featured the shear failure of the concrete tenon, due to the fact that the potential shear failure plane of the timber was restrained by the steel-plate of the testing set-up. The timber sheared parallel to the grain showed no obvious damage in the RSS(C) specimens.

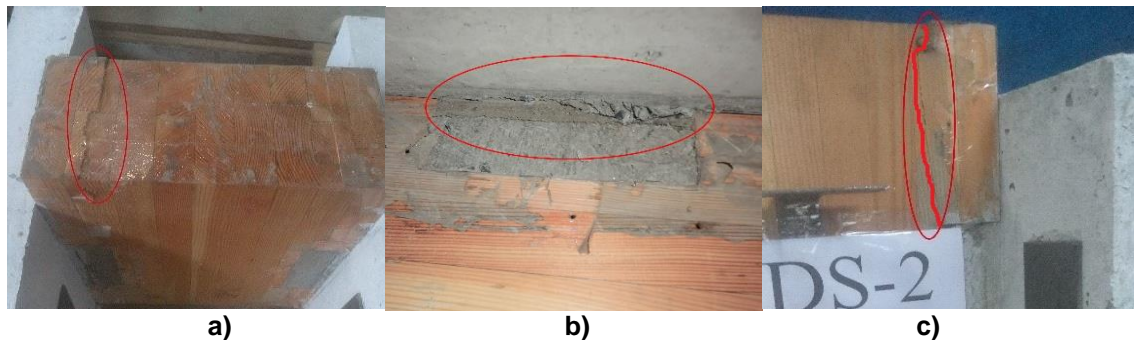
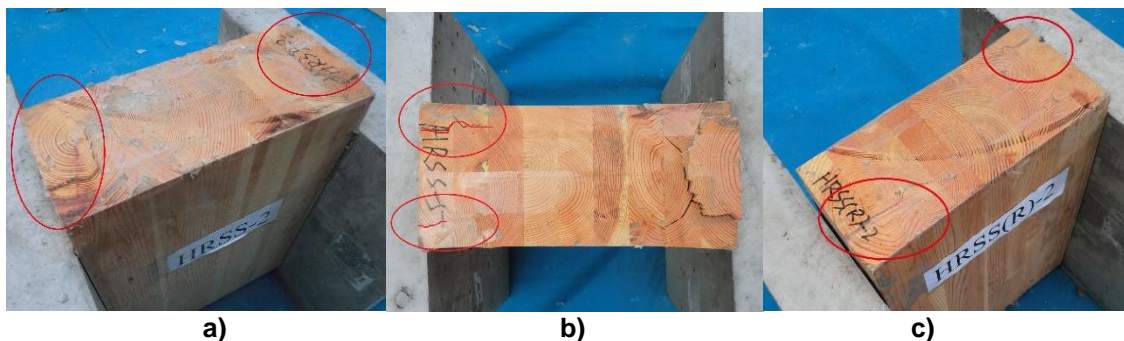


Fig. 5. Failure photographs of the Phase I push-out tests: a) the timber shear failure for RSS; b) the concrete shear failure for RSS(C); and c) the timber shear failure for RDS



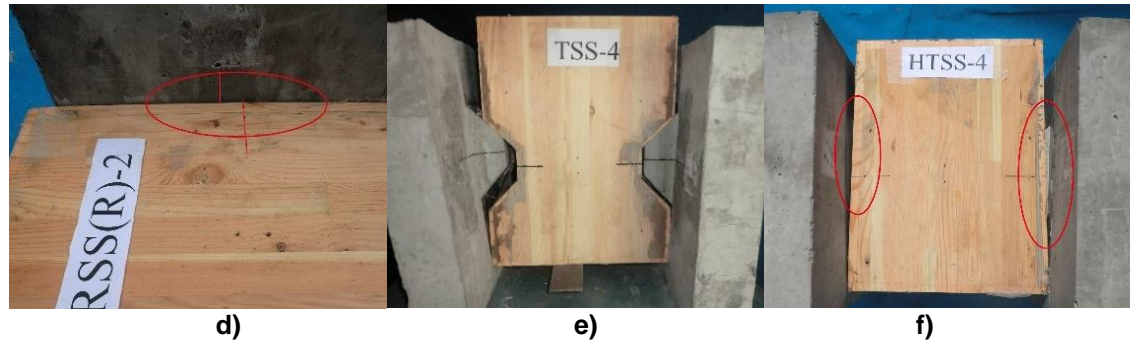


Fig. 6. Failure photographs of the Phase II push-out tests: a) the timber shear failure for HRSS; b) the timber shear and splitting failure for HRSS; c) the timber splitting failure for HRSS(R); d) the interface relative slip; e) the separation between the concrete and timber for the TSS specimens; and f) the separation between the concrete and timber for the HTSS specimens

The failure photographs of the specimens tested in Phase II are shown in Fig. 6. The HRSS specimens also showed shear failure of the timber block (Fig. 6a). Similar to the RSS and RDS specimens, the timber was sheared to failure along the outline of the deep notch. In addition, some HRSS samples also displayed timber splitting failure, as shown in Fig. 6b. As shown in Fig. 6c, the HRSS(R) specimens primarily displayed timber splitting failure. Both the HRSS and HRSS(R) specimens featured evident interfacial slip at the collapse limit state, as shown in Fig. 6d. Figure 6e and 6f displayed the typical failure modes of the TSS and HTSS specimens, respectively. For the TSS specimens, the concrete tenon evidently slipped out from the timber notch, and obvious separation between the concrete slab and the timber component occurred. These failure modes for the HTSS specimens were relatively slighter. The constraint of the lateral timber friction made considerable contributions to preventing the slipping out of the concrete for the HTSS specimens.

Load-Slip Behaviours

Load-slip curves

The load-slip behaviours of the push-out specimens are displayed in Fig. 7a through 7g, and the comparisons of the average curves are depicted in Fig. 7h. The testing loads in Fig. 7 include the total carrying loads of the two shear planes. The main discussions are summarized as follows: (1) Comparing RSS and RSS(C) specimens, loading constraint conditions showed evident influences on the ultimate bearing capacity. While the loaded ends of the timber were wholly restrained by the steel-plate, the shear strengths of the connection evidently improved due to the fact that the failure mode was concrete shear failure instead of timber shear failure; (2) Increasing the screw number in the notch led to a certain improvement in the ultimate bearing capacity. The failure mode and deformation ability were not improved; (3) HRSS and HRSS(R) specimens showed an improvement in the ultimate bearing capacity compared to the RSS ones. The residual bearing capacity and deformation capacity of the deep notch connection were obviously improved due to the increase in total width of the timber sheared and the application of reinforcement screws; (4) Compared with the specimens with rectangular notches, TSS and HTSS samples showed better post-yield bearing capacity and ultimate deformation ability.

Summary of testing results

Table 3 displays a summary of the testing results of two shear interfaces, in which the ultimate bearing capacity (F_u) was determined as the failure load of the tested specimens; the yield load (F_y), and the values of ultimate slip s_u and yield slip s_y were determined according to EN standard 12512 (2001). The slip moduli (K_s) were calculated in accordance with EN standard 26891 (1991).

From Table 3, the primary discussions can be summarized as follows: (1) Compared with the RSS samples, the ultimate and yield bearing capacities of the RSS(C) samples increased by 81% and 73%, respectively, which demonstrated that the concrete tenon showed superior bearing capacity compared to the timber in shear. Therefore, it is necessary to reinforce the weak timber block component in HNS connections; (2) RDS specimens showed an obvious improvement in the ultimate bearing capacity and yield load compared to the RSS samples due to the increase in the screw number, increasing by 31% and 20%, respectively; (3) HRSS specimens showed an approximately improvement of 24% compared to the RSS specimens compared to the shear strength due to the shear width increasing by 37%.

The ultimate slip and yield slip were also obviously improved compared with the RSS samples; (4) The self-tapping screw reinforcement provided a slight influence on the ultimate bearing capacities. However, the yield load and ultimate deformation capacity of the HRSS(R) specimens were greatly improved compared with the HRSS samples due to the reinforcement action of the VGZ7140 screws.

In terms of the slip moduli, the primary discussions can be summarized as follows: (1) The loading constraint conditions and the screw number have slight influences on the slip moduli, which was found by analyzing the results of the Phase I tests. The differences between the different groups may be caused by reasonable material differences; (2) Compared with the RSS specimens, the HRSS samples showed a decrease of approximately 50% in the slip modulus, due to the reduction of the notch width, which demonstrated that the notch width had an important effect on the slip moduli; (3) Due to the application of the self-tapping screw as reinforcement, the slip moduli of the HRSS(R) specimens slightly improved. The values of K_s increased by approximately 6.4%. The coefficient of variation (COV) for the HRSS(R) specimens obviously decreased. Apparently, the self-tapping screw for the sheared timber component can improve the slip moduli and the stability of shear performances; (4) the TSS and HTSS specimens showed an obvious decrease in the slip moduli compared to the specimens with rectangular notches.

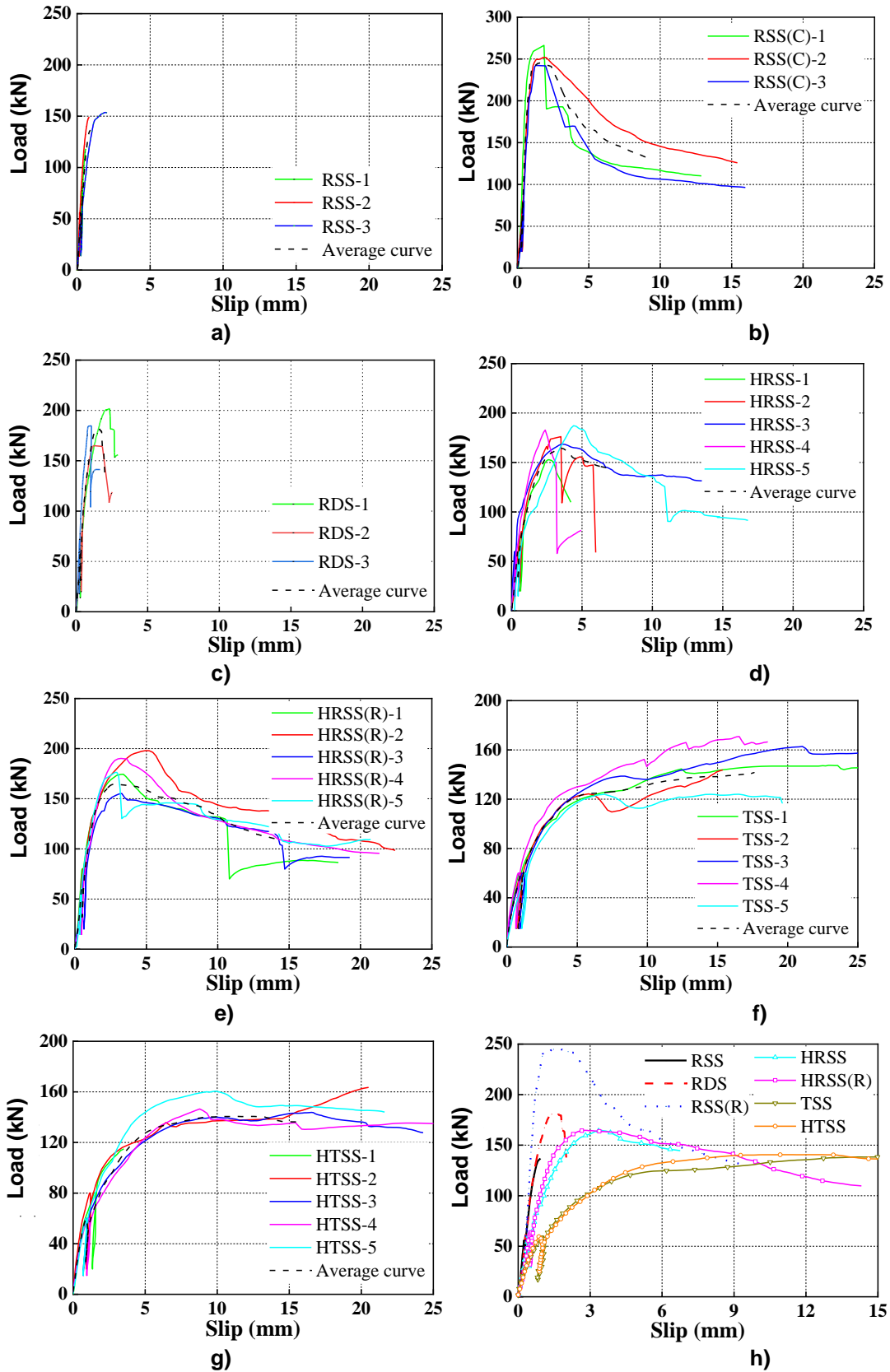


Fig. 7. Load-slip curves of the push-out specimens: a) group RSS; b) group RSS(C); c) group RDS; d) group HRSS; e) group HRSS(R); f) group TSS; g) group HTSS; and h) a comparison of all the samples

Table 3. Primary Results of the Push-out Tests

Groups	No.	F_u (kN)		F_y (kN)		s_u (mm)		s_y (mm)		K_s (kN/mm)	
		Indiv.	Av.	Indiv.	Av.	Indiv.	Av.	Indiv.	Av.	Indiv.	Av.
RSS	1	118.2	140.3 (12%)	114.6	121.3 (7%)	0.59	1.13 (52%)	0.55	0.67 (36%)	266.7	307.2 (51%)
	2	149.0		115.3		0.84		0.45		480.0	
	3	153.6		134.1		1.95		1.00		175.0	
RSS(C)	1	266.3	253.4 (4%)	218.7	210.0 (5%)	1.86	1.73 (18%)	0.63	0.79 (19%)	406.1	273.8 (42%)
	2	251.7		194.7		2.02		0.75		212.2	
	3	242.3		216.6		1.30		0.99		203.0	
RDS	1	200.5	183.3 (10%)	119.1	145.2 (13%)	2.35	1.48 (43%)	0.71	0.78 (12%)	207.4	259.7 (35%)
	2	165.0		150.3		1.23		0.92		208.7	
	3	184.3		166.2		0.85		0.72		363.1	
HRSS	1	152.7	173.5 (7%)	126.6	115.7 (18%)	3.64	5.04 (46%)	1.68	1.22 (38%)	124.6	158.9 (26%)
	2	176.2		141.8		3.50		1.82		127.0	
	3	168.5		98.9		7.60		0.56		226.4	
	4	182.7		126.7		2.39		1.09		168.1	
	5	187.2		84.4		8.09		0.97		148.5	
HRSS(R)	1	174.5	178.7 (8%)	125.3	132.8 (10%)	7.08	6.68 (29%)	1.08	1.35 (20%)	184.8	169.0 (23%)
	2	198.0		134.4		7.12		1.30		165.0	
	3	155.3		124.5		9.25		1.42		117.0	
	4	189.7		157.7		6.64		1.81		156.7	
	5	176.2		121.9		3.32		1.12		221.4	
TSS	1	144.6	136.8 (9%)	84.4	94.6 (8%)	15.0	15.0 (0%)	1.94	2.43 (15%)	63.8	53.2 (19%)
	2	124.3		96.4		15.0		2.46		53.0	
	3	138.7		103.0		15.0		3.06		43.4	
	4	152.3		101.4		15.0		2.19		63.2	
	5	124.0		87.8		15.0		2.48		42.6	
HTSS	1	115.0	145.7 (7%)	103.3	100.0 (7%)	15.0	15.0 (0%)	2.44	2.55 (19%)	48.6	57.7 (14%)
	2	135.8		100.1		15.0		2.01		60.7	
	3	140.0		86.7		15.0		2.10		61.4	
	4	146.5		100.5		15.0		3.35		50.4	
	5	160.6		109.3		15.0		2.83		67.2	

Note: the ultimate strength of HTSS-1 was not considered due to the malfunction of the testing device; percentage values denote the coefficient of variation (COV)

Ductility Performance

The ductility of the shear connections greatly influences the feasibility of their application in TCC structures, which reflects the ability of the shear connection to sustain the relatively large slip in the plastic range without an obvious reduction in their strength. Two methods were adopted to evaluate the ductility of the shear connection, which were recommended by EN standard 12512 (2001) and Deam *et al.* (2008), respectively.

Deam *et al.* (2008) recommended that the shear connection can be defined as brittle failure if it cannot sustain a slip of 10 mm without a decrease in strength greater than 20% of the ultimate bearing capacity, while other cases can be defined as ductile. As depicted in Eq. 1,

$$D_1 = \frac{F_u - F_{10}}{F_u} \times 100\% \quad (1)$$

where F_u is the ultimate bearing capacity of shear connection and F_{10} is the testing load at the slip of 10 mm. The connection can be defined as ductile when D_1 is no larger than 20%.

The evaluation method provided by EN standard 12512 (2001) was also adopted to estimate the ductility factor of the joints, as shown in Eq. 2,

$$D_2 = \frac{s_u}{s_y} \quad (2)$$

where s_u and s_y are the ultimate slip and yield slip, respectively, which were determined based on the load-slip curves shown in Fig. 7 according to EN standard 12512 (2001).

The ductility results are shown in Table 4, in which the maximum interface relative slips were also displayed to reflect the deformation ability of the shear connections. The specimens in groups RSS and RDS were defined as having brittle failure and showed weak deformability. The trapezoidal notched connections with screws showed ductility behavior with the factors of 6.17 and 5.88. The slant notch could increase the ductility of the connections and improve the stress mechanism of the deep notched connections. However, a large slant angle will lead to an opening gap, which leads to a decrease in the slip moduli. Although D_1 is larger than 20% for the HTSS(R) specimens, it still could be regarded as ductile failure, as the ductility factor D_2 reached approximately 4.95. The ductility performance and deformation ability were apparently improved thanks to the application of the self-tapping screw reinforcement.

Table 4. Ductility Factors and Maximum Slip

Groups	D_1	D_2	Maximum Slip (mm)
RSS	100%, Brittle	1.67	1.2
RSS(C)	100%, Brittle	2.25	14.3
RDS	100%, Brittle	1.90	2.4
HRSS	69.3%, Brittle	4.13	9.0
HRSS(R)	24.4%, Brittle	4.95	15.0
TSS	Ductile	6.17	15.0
HTSS	Ductile	5.88	15.0

Slip Modulus Models

Table 3 shows that the slip moduli of the HRSS and HRSS(R) connections decreased by approximately 50% as the width of concrete tenon decreased by 37%. Apparently, the notch width directly influenced the slip modulus of the HNS connection. As to the effects of the notch depth, according to the report by Kudla (2015), the slip modulus of a notched connection increases as the notch depth increases. In addition, from the investigations of Jiang *et al.* (2020) and Zhang *et al.* (2020), it can be found as the notch depth increases, the initial slip moduli tend to reach the upper limit. This is because the shallow notch (10 mm to 20 mm) primarily showed timber crushing, as outlined in Kudla (2017) and Thai *et al.* (2020), while a deep notch showed a shear failure mechanism (as shown in Fig. 5 and Fig. 6), as described by relevant investigations (Xie *et al.* 2017; Jiang *et al.* 2020; Zhang *et al.* 2020). As to the effects of the timber length in front of the notch in terms of the slip moduli, conclusions in existing investigations are inconsistent. Some investigations stated there was no obvious effect (Jiang and Crocetti 2019; Zhang *et al.* 2020), while some studies showed either a slight improvement (Thai *et al.* 2020) or an approximately linear proportion improvement (Michelfelder 2006; Mönch and Kuhlmann 2018), with an increase in length of the timber sheared. Based on the above analysis, simplified methods to evaluate the slip modulus of deep notch connections with pure

shearing effect by referring to the component method concept are proposed in Eq. 3 (model 1) and Eq. 4 (model 2 and model 2*),

$$\frac{1}{K_s} = \frac{1}{G_w \sqrt{l_w b_n}} + \frac{1}{G_c \sqrt{l_c b_n}} \tag{3}$$

$$\frac{1}{K_s} = \frac{1}{G_w b_n} + \frac{1}{G_c b_n} \tag{4}$$

where G_w is the shear modulus of the timber, G_c is the shear modulus of the concrete; b_n is notch width, and l_w and l_c are the shear length of the timber and concrete, respectively.

In the proposed models, it was considered that the shear moduli of a deep notch connection were determined by two springs in series, which were provided by the timber shear plane and concrete shear plane, respectively. For the timber shear modulus, two conditions were provided, which were determined as 650 MPa (Model 1 and Model 2) according to the characteristic value in EN standard 14080 (2013) for a conservative calculation and 930 MPa (Model 2*) for the experimental conditions (Ukyo *et al.* 2010).

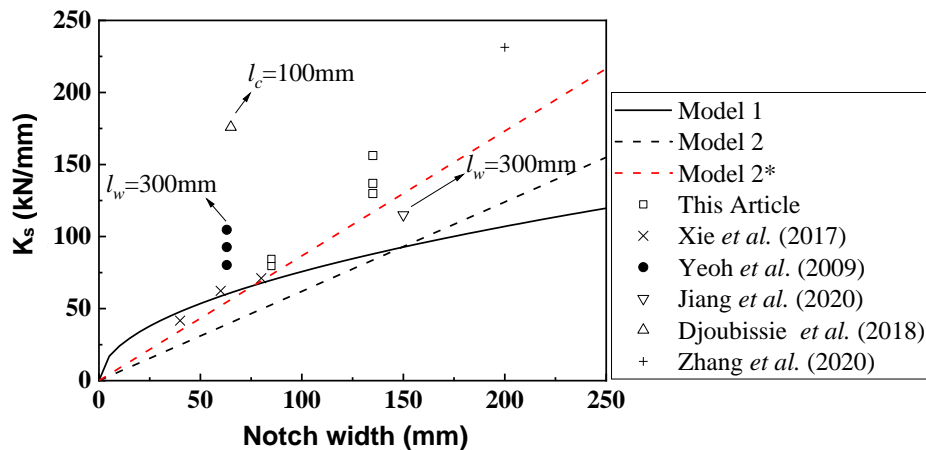


Fig. 8. Slip moduli of one notch depending on the notch width

Table 5. Experimental Results of Existing Investigations

References	h (mm)	l_c (mm)	l_w (mm)	Modulus of Elasticity of Timber (GPa)	Concrete Grades
Xie <i>et al.</i> (2017)	50	150	250	Density, 562.5 kg/m ³	C30
Yeoh <i>et al.</i> (2009)	50	150	300	11.3 (LVL)	C35
Jiang <i>et al.</i> (2020)	50	150	300	10.7	C30
Djoubissie <i>et al.</i> (2018)	40	100	150	12.2	C25
Zhang <i>et al.</i> (2020)	40	150	250	12.0	C50

Note: h denotes the depth of notches; l_c denote the notch length, *i.e.* the shear length of the concrete; l_w is the shear length of the timber. The timber used in Yeoh *et al.* (2009) was laminated veneer lumber (LVL).

The comparisons between the model values and the testing results of this study and other investigations with ordinary concrete, similar notch depth, and length are shown in Fig. 8, and the detailed information about notched type connections in existing references are displayed in Table 5. The accuracy of model 1 rapidly declined as the notch width increased, which is not recommended for TCC floors. Model 2* showed reliable evaluation values while model 2 displayed slightly conservative results. The experimental results of

Djoubissie *et al.* (2018) are much larger than the other results, which may be caused by the application of hardwood with a density of 690 kg/m^3 . In addition, in EN standard 1995-1-1:2004/A2:2014 (2014), a slip modulus of 1500 N/mm for a 1 mm wide deep notch (greater than 30 mm) was provided. This reference value overestimated the slip modulus of deep notch connection for T-shaped TCC beams due to a relatively small notch width. The predicted slip moduli based on Models 2 and 2* are approximately 40% and 55% of the reference value of 1500 N/mm with a 1 mm width.

Further investigations will focus on the long-term performances of notched connections and their corresponding TCC beams by considering the notch dimensions and prefabricated assembly method. Preliminary studies demonstrated that the connection shear performance and precast concrete members greatly influence the creep coefficients of TCC structures (Shi *et al.* 2020, 2021a). The influences of the related parameters on the long-term performances of TCC structures with HNS connections will be studied further.

CONCLUSIONS

1. The loading constraint conditions showed obvious effects on the failure modes and shear strength of HNS connections. The timber component sheared showed a relatively weak bearing capacity and more obvious brittle failure compared with the concrete tenon reinforced with screws.
2. The notch width greatly influenced the slip moduli while the timber area sheared effected the shear strength. Comparing the HRSS samples with the RSS samples, the ultimate bearing capacity increased by 24% due to the timber shear width increasing by 37%, while the slip moduli decreased by approximately 50%, with the notch width decreasing by 37%.
3. Self-tapping screw reinforcement provided a slight improvement in terms of the shear strength and slip moduli. However, the deformation ability and brittle shear failure of the timber were improved apparently. The ductility factor of the HRSS(R) samples reached 4.95, approaching ductile failure.
4. Slip modulus models were provided for vertical deep notches. The calculation results of the models provided were in agreement with the experimental results, which have certain reference importance for the T-shaped TCC structures in actual design.

ACKNOWLEDGMENTS

The authors are grateful for the support of the National Natural Science Foundation of China (Grant. No. 51878344) and the Postdoctoral Foundation of Jiangsu Province (Grant 2021K128B).

REFERENCES CITED

ASTM D 905-08 (2013). "Standard test method for strength properties of adhesive bonds in shear by compression loading," ASTM International, West Conshohocken, PA.

- ASTM F1575-17 (2017). “Standard test method for determining bending yield moment of nails,” ASTM International, West Conshohocken, PA.
- Auclair, S. C. (2020). *Design Guide for Timber-Concrete Composite Floors in Canada*, FP Innovations, Pointe-Claire, Quebec, Canada.
- Auclair, S. C., Sorelli, L., and Salenikovich, A. (2016). “A new composite connector for timber-concrete composite structures,” *Construction and Building Materials* 112, 84-92. DOI: 10.1016/j.conbuildmat.2016.02.025
- Boccardo, L., Steiger, R., Zweidler, S., and Frangi, A. (2017a). “Analysis of shear transfer and gap opening in timber-concrete composite members with notched connections,” *Materials and Structures* 50(5), 1-15. DOI: 10.1617/s11527-017-1098-3
- Boccardo, L., Zweidler, S., Steiger, R., and Frangi, A. (2017b). “Calculation model to assess the structural behavior of LVL-concrete composite members with ductile notched connection,” *Engineering Structures* 153, 106-117. DOI: 10.1016/j.engstruct.2017.10.024
- Deam, B. L., Fragiaco, M., and Buchanan, A. H. (2008). “Connections for composite concrete slab and LVL flooring systems,” *Materials and Structures* 41(3) 495-507. DOI: 10.1617/s11527-007-9261-x
- Dias, A. M. P. G., Kuhlmann, U., Kudla, K., Mönch, S., and Dias, A. M. A. (2018a). “Performance of dowel-type fasteners and notches for hybrid timber structures,” *Engineering Structures* 171, 40-46. DOI: 10.1016/j.engstruct.2018.05.057
- Dias, A. Schänzlin, J., and Dietsch, P. (2018b). *Design of Timber-concrete Composite Structures* (COST Action FP1402/WG 4), European Cooperation in Science and Technology (COST), Brussels, Belgium.
- Djoubissie, D. D., Messan, A., Fournely, E., and Bouchaïr, A. (2018). “Experimental study of the mechanical behavior of timber-concrete shear connections with threaded reinforcing bars,” *Engineering Structures* 172, 997-1010. DOI: 10.1016/j.engstruct.2018.06.084
- EN 12512 (2001). “Timber structures – Test methods - Cyclic testing of joints made with mechanical fasteners,” European Committee for Standardization, Brussels, Belgium.
- EN 14080 (2013). “Timber structures – Glued laminated timber and glued solid timber – Requirements,” European Committee for Standardization, Brussels, Belgium.
- EN 1995-1-1:2004/A2:2014 (2014). “Eurocode 5: Design of timber structures – Part 1-1: General – Common rules and rules for buildings,” European Committee for Standardization, Brussels, Belgium.
- EN 26891 (1991). “Timber structures – Joint made with mechanical fasteners – General principles for the determination of strength and deformation characteristics,” European Committee for Standardization, Brussels, Belgium.
- EN 408 (2009). “Timber structures – Structural timber and glued laminated timber - Determination of some physical and mechanical properties,” European Committee for Standardization, Brussels, Belgium.
- ISO 3347 (1976). “Wood – Determination of ultimate shear stress parallel to grain,” International Organization for Standardization, Geneva, Switzerland.
- Jiang, Y., and Crocetti, R. (2019). “CLT-concrete composite floors with notched shear connectors,” *Construction and Building Materials* 195, 127-139. DOI: 10.1016/j.conbuildmat.2018.11.066
- Jiang, Y., Hu, X., Hong, W., Zhang, J., and He, F. (2020). “Experimental study on notched connectors for glulam-lightweight concrete composite beams,” *BioResources* 15(2), 2171-2180. DOI: 10.15376/biores.15.2.2171-2180

- Kudla, K. (2015). *Notched Connections for TCC Structures as Part of the Standard* (COST Action FP1402), European Cooperation in Science and Technology (COST), Brussels, Belgium.
- Kudla, K. (2017). *Kerven als Verbindungsmittel für Holz-Beton-Verbundstraßenbrücken [Notches as connections for timber-concrete-composite road bridges]*, Ph.D. Dissertation, Institute of Structural Design, University of Stuttgart, Stuttgart, Germany.
- Lamothe, S., Sorelli, L., Blanchet, P., and Galimard P. (2020). “Engineering ductile notch connections for composite floors made of laminated timber and high or ultra-high performance fiber reinforced concrete,” *Engineering Structures* 211, 1-12. DOI: 10.1016/j.engstruct.2020.110415
- Michelfelder, B. C. (2006). *Trag- und Verformungsverhalten von Kerven bei Brettstapel-Beton-Verbunddecken [Load-bearing and deformation behaviours of notches for Brettstapel(Dowel Laminated Timber, DLT)-concrete-composite slabs]*, Ph.D. Dissertation, Institute of Structural Design, University of Stuttgart, Stuttgart, Germany.
- Mönch, S., and Kuhlmann, U. (2018). “Investigation on the effects of geometry in timber-concrete composite push-out tests with notched connections,” in: *Proceeding of the 15th World Conference of Timber Engineering 2018 (WCTE 2018)*, 20-23 August, Seoul, South Korea, B2CON-05-03.
- Müller, K., and Frangi, A. (2021). “Micro-notches as a novel connection system for timber-concrete composite slabs,” *Engineering Structures* 245, 1-10. DOI: 10.1016/j.engstruct.2021.112688
- Rothoblaas (2019). *Screws and Connectors for Wood*, Rothoblaas Srl, Cortaccia (BZ), Italy.
- Shi, B., Liu, W., Yang, H., and Ling, X. (2020). “Long-term performance of timber-concrete composite systems with notch-screw connections,” *Engineering Structures* 213, 1-11. DOI: 10.1016/j.engstruct.2020.110585
- Shi, B., Liu, W., and Yang, H. (2021a). “Experimental investigation on the long-term behaviour of prefabricated timber-concrete composite beams with steel plate connections,” *Construction and Building Materials* 266(Part A), 1-12. DOI: 10.1016/j.conbuildmat.2020.120892
- Shi, B., Liu, W., Yang, H., Tao, H., and Wang, C. (2021b). “Experimental behaviour of timber-concrete composite beams with notched-screw connections,” *Journal of Building Structures* 42(10), 104-113. DOI: 10.14006/j.jzjgxb.2019.0864
- Thai, M. V., Ménard, S., Elachachi, S. M., and Galimard, P. (2020). “Performance of notched connectors for CLT-concrete composite floors,” *Buildings* 10(7), 1-21. DOI: 10.3390/buildings10070122
- Ukyo, S., Ido, H., Nagao, H., and Kato, H. (2010). “Simultaneous determination of shear strength and shear modulus in glued-laminated timber using a full-scale shear block specimen,” *Journal of Wood Science* 56, 262-266. DOI: 10.1007/s10086-009-1083-8
- Xie, L. He, G., Wang, X., Gustafsson, P. J., Crocetti, R., Chen, L., Li, L., and Xie, W. (2017). “Shear capacity of stud-groove connector in glulam-concrete composite structure,” *BioResources* 12(3), 4690-4706. DOI: 10.15376/biores.12.3.4960-4706
- Yeoh, D., Fragiacomò, M., Buchanan, A., and Gerber, C. (2009). “Preliminary research towards a semi-prefabricated LVL-concrete composite floor system for the Australasian market,” *Australian Journal of Structural Engineering* 9(3), 225-240. DOI: 10.1080/13287982.2009.11465025

Yeoh, D., Fragiacomio, M., Franceschi, M. D., and Buchanan, A. (2010). "Experimental tests of notched and plate connectors for LVL-concrete composite beams," *Journal of Structural Engineering* 137(2), 261-269. DOI: 10.1061/ASCEST.1943-541X.0000288

Zhang, L., Chui, Y. H., and Tomlinson, D. (2020). "Experimental investigation on the shear properties of notched connections in mass timber panel-concrete composite floors," *Construction and Building Materials* 234, 1-14. DOI: 10.1016/j.conbuildmat.2019.117375

Article submitted: November 15, 2021; Peer review completed: January 29, 2022;
Revised version received and accepted: February 10, 2022; Published: February 24, 2022.
DOI: 10.15376/biores.17.2.2259-2274